

PACS numbers: 28.60.+s; 32.80.Fb; 42.62.–b
DOI: 10.1070/QE2003v033n07ABEH002465

On laser rare-isotope separation

A.N. Tkachev, S.I. Yakovlenko

Abstract. **A brief review on laser separation of rare ytterbium and palladium isotopes by selective photoionisation is presented. The ^{168}Yb isotope enrichment is performed using the optical scheme proposed by A.M. Prokhorov and co-workers in 1991. The kinetic model of selective photoionisation is described in detail and the production of highly enriched ^{168}Yb isotopes in weight quantities is reported (up to 90 % – 95 % in a plasma, up to 62 % on a collector, and up to 45 % in a wash solution). The rate of production of enriched ytterbium achieves 5 – 10 mg h^{-1} (more that 1 g per month). The results of theoretical and experimental studies of selective photoionisation of palladium are also presented. A substantial enrichment of different palladium isotopes is achieved: ^{102}Pd – up to 18 % (the natural content is 1 %), ^{104}Pd – up to 70 % (11.4 %), and ^{105}Pd – up to 60 % (22.33 %). The kinetics of selective ionisation of palladium is analysed using new experimental data on the fine structure and hyperfine splitting of the terms.**

Keywords*: laser isotope separation, selective photoionisation, autoionisation states.*

1. Introduction

It is known that Alexander Mikhailovich Prokhorov actively supported the studies devoted to laser isotope separation [1 – 4]. Being an Academician-Secretary of the Division of General Physics and Astronomy, Russian Academy of Sciences, he stimulated these studies not only at the General Physics Institute, RAS, but also at other institutions in our country, in particular, at the Institute of Spectroscopy, RAS [5 – 7]. In this review, we describe the studies on laser separation of rare isotopes by selective photoionisation, which resulted in the commercially efficient production of isotopes (see reviews [8 – 10]). Our main concern in this review is with ytterbium and palladium; however, many of the problems considered here are common for other rare isotopes as well.

Foundations of the method. The idea and first developments of the method of laser isotope separation based on selective photoionisation belong to V.S. Letokhov [7, 11]. Laser selective photoionisation ionisation of isotopes is often called atomic vapour laser isotope separation (AVLIS) in Western research papers; we will, however use here the abbreviation LIS (laser isotope separation).

A simplified scheme of the LIS method is shown in Fig. 1. The isotope separation process consists of several stages.

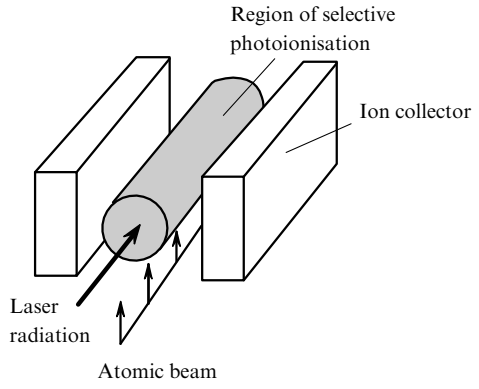

Figure 1. Scheme of the method for laser isotope separation.

(1) A vapour of a working element is obtained from a solid-state phase. This vapour contains the natural mixture of isotopes. High-melting elements, for example, uranium and gadolinium, are evaporated by an electron beam. Low-melting metals (for example, ytterbium) are heated in an oven.

(2) The obtained vapour is ionised by radiation from several lasers. To ionise predominantly a required isotope, the laser linewidth should be very narrow and should be very precisely tuned (often with an accuracy to the seventh decimal place in the wavelength) to the transition in the isotope. Laser radiation should be also sufficiently stable.

(3) Ions having an enriched isotopic composition are extracted from the vapour and are transported to a collector using an electric field or its combinations with a magnetic field. Then, the matter is processed by means of long known and well-developed chemical methods.

Two directions of LIS. There exist two main directions in the development of this method for stable isotopes: the production of comparatively large amounts (of the order of a ton per year) of a weakly enriched isotope (for example, ^{235}U) for nuclear power engineering and the production of highly enriched isotopes in much lower amounts for medicine.

A.N. Tkachev, S.I. Yakovlenko A.M. Prokhorov General Physics Institute, Russian Academy of Sciences, ul. Vavilova 38, 119991 Moscow, Russia

Received 9 January 2003
Kvantovaya Elektronika **33** (7) 581 – 592 (2003)
Translated by M.N. Sapozhnikov

LIS can be also used to study radioactive isotopes, in particular, to obtain isobaric-pure beams of short-lived radioactive isotopes [12]. However, we discuss here the studies aimed at the production of commercial amounts of stable isotopes.

The LIS programs were initiated in the USSR and USA in the mid-1970s. In the USA, the laser separation of uranium isotopes was mainly performed at the Lawrence Livermore National Laboratory, where considerable successes were reported. However, the laser method for producing nuclear fuel is still much more expensive than the usual method. In any case, isotopes produced by the laser method have not appeared so far in the world market. At present these studies are postponed. Their cost have amounted to approximately two billion dollars.

In the USSR, resonance laser ionisation of atoms and isotope separation were studied at the General Physics Institute, RAS, and the Institute of Spectroscopy, RAS, and the research on separation of uranium isotopes was mainly performed at the I.V. Kurchatov Atomic Energy Institute (now Kurchatov Federal Scientific Center). At present the LIS method is being actively developed in France and Japan.

The outlook for the development of LIS methods for atomic power reactors is doubtful. The matter is that, beginning from the 1950s, the gas centrifugal separation method have been used in our country for commercial production of isotopes, and it seems unlikely that LIS will be capable of competing with centrifugal isotope separation in the near future.

However, the method of gas centrifuging can be applied only to elements having sufficiently stable gaseous chemical compounds. Otherwise, a rather expensive method of electromagnetic separation is used with which LIS can compete.

In our opinion, at present it is more promising to use LIS for producing highly enriched isotopes in moderate amounts (of the order of a few kilograms per year) for medicine.

Basic problems. The selective ionisation of many elements under laboratory conditions was demonstrated back in the 1970s. However, the task of producing weighable amounts of a highly enriched isotope, whose content in the natural mixture is low, gives rise to a number of new theoretical and technical problems. We list here only some of them.

(i) The necessity of the most efficient use of laser radiation. Laser radiation has a high quality and its production is quite expensive. However, the intensities of absorption of laser radiation at different transitions in an atomic vapour are substantially different. For example, laser radiation can be already absorbed almost completely at the first transition, whereas only one hundredth part of the incident radiation is absorbed at the third transition.

(ii) A complicated control of the ion-extraction process. Plasma produced upon photoionisation behaves often erratically in external electric and magnetic fields. More exactly, it is difficult to calculate its motion and even more difficult to provide the conditions under which the plasma behaviour will correspond to calculations.

(iii) Contamination of an ion collector. Even a very small amount of an evaporated material should not fall on the collector if the natural content of the required isotope is low. Of course, to prevent the entering of a beam of evaporated ions on the collector, a limiting aperture can be used. However, atoms in the beam collide with each other and can fall into the region of the geometrical shade.

The problems arising in the studies should be solved in combination rather than separately. For example, the design of a vapour source should take into account not only the problems of collector contamination and plasma transport but also provide the matching between the vapour density and the laser power. In addition, the Doppler velocity distribution of atoms in the vapour flow should correspond to the laser linewidth.

Moreover, even when these problems are solved in principle, one should not only calculate accurately the operating regime close to the optimal but also implement it in practice. At the same time, the operating regime of the facility is characterised by hundreds of different parameters. For example, each laser beam is specified not only by the laser frequency but also by the shape of the laser line, as well as by the characteristic rise and decay times of a laser pulse, the angles at which the laser beam is incident on a medium, and polarisation.

All this makes the laser separation of weighable amounts of initially low-content isotopes one of the most advanced technologies, in particular, technologies for producing ultrapure materials.

Separation of weighable amounts of ^{168}Yb. The investigations performed at the General Physics Institute, RAS and the LAD Research and Production Association (now IZO) were aimed at the production of gram amounts of the highly enriched isotope for medicine [13–19]. This problem is more scientific but requires less material expenditures, which significantly facilitates progress in this field. The ^{168}Yb isotope is one of the interesting examples of an expensive rare isotope. Its content in the natural mixture is only 0.14 %, whereas a mixture enriched up to 20 %–25 % is used. As a result, the cost of this isotope, according to the Oakridge price list, amounts to more than 300 thousands dollars per gram (note, however, that the prices in this price list are nearly twice as large as real prices in the market). This isotope is used in medicine for diagnostics of defects of the cardiac muscle and in the cancer treatment.

A scheme for the selective three-step ionisation of ytterbium was proposed in 1991 by A.M. Prokhorov, B.B. Krynetskii, and V.A. Mishin [4] (Fig. 2). This scheme is attractive because selective ionisation can be performed using visible radiation from tunable dye lasers pumped by copper vapour lasers. Selective excitation occurs at the second transition at 581.067 nm.

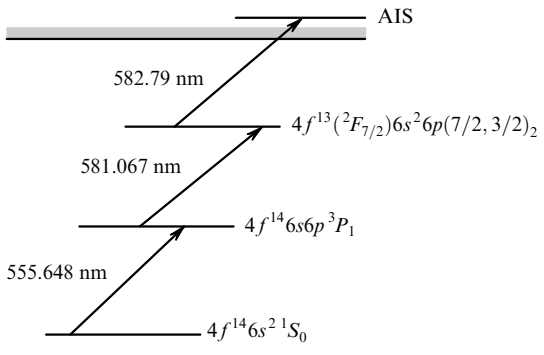

Figure 2. Scheme for three-step photoionisation of an ytterbium atom.

However, to implement this scheme, a number of important scientific and technical problems should be solved, which appeared neither in laboratory studies nor in the research that was not directly intended for a profitable isotope production. Because our studies were initially aimed at the commercial production of weighable amounts of the rare isotope, they are substantially different both from the studies devoted to the production of a nuclear fuel for power reactors and from laboratory developments.

On the one hand, we have managed to use comparatively small-size low-energy setups and to avoid the problems related to the electron-beam evaporation of materials. On the other hand, because of a low content of the required isotope, the problems related to the selectivity and efficiency of photoionisation within a comparatively large volume [20 – 22] and to the contamination of the collector during the formation of a vapour flow [23 – 29] were aggravated. At the same time, the necessity of producing the rare isotope in weighable amounts dramatises these problems because a considerable volume charge appears during the extraction of ions [30 – 35]. All these problems were solved simultaneously rather than separately, using computer simulations.

The LIS method was developed to a qualitatively new level in papers [13 – 19] (see also reviews [8 – 10]). All the above-mentioned key problems of the laser separation of weighable amounts of the isotope with the initial low content in the natural mixture have been solved. Below, we present a brief review of these studies, a special attention being paid to the choice of the photoionisation scheme and to some problems that were insufficiently discussed in [8 – 10].

Separation of weighable amounts of ^{102}Pd. Another isotope of commercial interest is ^{102}Pd, whose content in the natural mixture is 1.02 %. According to the Oakridge price list, the cost of the 90-% enriched ^{102}Pd is 700 thousands dollars per gram. It is reasonable to use the experience accumulated in producing ^{168}Yb for separating ^{102}Pd in weighable amounts.

The above-mentioned problems involved in the separation of a rare isotope in weighable amounts exist for ^{102}Pd as well. In addition, a number of additional problems inherent in palladium only appear:

(i) The optical scheme for the selective photoionisation of ^{102}Pd has not been studied theoretically and experimentally so far and, moreover, even did not exist until recently. Only the scheme for the output product enrichment by the ^{105}Pd and ^{107}Pd isotopes was considered [36, 37].

(ii) The characteristic isotope shifts in palladium are much smaller than these in ytterbium. In addition, no reliable experimental data were available on the isotopic and hyperfine structures of the $4d^9 5p\,^3P_1$ level, which is most convenient for LIS.

(iii) The frequencies of electronic transitions in palladium lie in the UV region. At the same time, tunable visible dye lasers pumped by copper vapour lasers are at present most convenient sources for commercial LIS. Therefore, it is necessary to use frequency doubling, which substantially complicates the technological process.

(iv) The evaporation temperature of palladium is higher than that of ytterbium. This significantly complicates the design of an oven.

The principal possibility of commercial production of ^{102}Pd in weighable amounts was studied in papers [38 – 41]. More accurate data on the isotopic and hyperfine structures of palladium terms were recently reported in paper [42]. Below, we present the theoretical analysis of the possibility of selective photoionisation of palladium taking the recent data into account.

2. Laser separation of ytterbium isotopes

2.1 Kinetic model of selective photoionisation

The choice of excited states. The authors of papers [14 – 19] (see also Refs [8 – 10]) used the three-step photoionisation of ^{168}Yb via the autoionisation state (AIS), which was proposed in Ref. [4] (Fig. 2)

$$|4f^{14}6s^2\,{}^1S_0\rangle \xrightarrow{\lambda=555.648\ \mathrm{nm}} |4f^{14}6s6p\,{}^3P_1\rangle \xrightarrow{581.067\ \mathrm{nm}}$$

$$|4f^{13}(^2F_{7/2})6s^2 6p(7/2,3/2)_2\rangle \xrightarrow{582.79\ \mathrm{nm}} \mathrm{AIS}. \qquad (1)$$

This scheme uses dye lasers pumped by copper vapour lasers. Selection is performed at the second transition. Let us substantiate in more detail the choice of this scheme.

Consider Rhodamine 6G dye lasers pumped by a copper vapour laser at 510.554 and 578.213 nm. We assume that the dye lasers are tunable between 540 and 600 nm, this tuning range being somewhat broader than in reality. The emission linewidths of the copper laser correspond to photon energies 19 587 and 17 295 cm^{-1}, and the corresponding frequency tuning range of the Rhodamine 6G laser is 18 520 – 16 600 cm^{-1}.

The ground state of Yb (the first level of the scheme) has the $4f^{14}6s^2\,{}^1S_0$ configuration (even level). The transition from this level can occur to an odd state with $J = 1$. The energies of the four lower excited states $4f^{14}\,6s6p\,{}^3P_0$, $4f^{14}\,6s6p\,{}^3P_1$, $4f^{14}\,6s6p\,{}^3P_2$, and, $4f^{13}5d6s^2$ $(7/2,\ 3/2)_2$ of Yb are 17 288.44, 17 992.0, 19 710.39, and 23 188.52 cm^{-1}, respectively. The energies of all the three levels $4f^{14}6s6p\,{}^3P_{0,1,2}$ are suitable for using them as the second level in the scheme; however, according to the selection rules, only the $4f^{14}\,6s6p\,{}^3P_1$ level can be used. The isotopic and hyperfine structure (HFS) of the $^1S_0 \rightarrow {}^3P_1$ transition cannot provide the high excitation selectivity of ^{168}Yb at this transition because of blending of the absorption lines of the ^{168}Yb isotope with the lines of odd isotopes (Table 1).

The third level of the ionisation scheme should be even and should have the total momentum $J = 0$, 1, or 2. The energy of this level should lie in the range between 34 592 and 36 512 cm^{-1} or should be exactly equal to 35 287 or 37 579 cm^{-1} (if we use directly radiation from a copper vapour laser).

Table 1. Parameters of the $6\,{}^3P_1 \rightarrow 6\,{}^1S_0$ transitions taking into account the isotopic and hyperfine structures of Yb isotopes (experimental data [4]; the error is $\sim$ 10 MHz).

A	$F' - F$	$\Delta\nu$/MHz
173	7/2 – 5/2	−2409
171	1/2 – 1/2	−2136
176	1 – 0	−948
174	1 – 0	0
172	1 – 0	993
170	1 – 0	2283
173	5/2 – 5/2	2301
168	**1 – 0**	**3636**
173	3/2 – 5/2	3804
171	3/2 – 1/2	3816

Note: The ^{168}Yb isotope of most practical interest is presented in bold.

In the energy range between 34 500 and 38 000 cm^{-1}, the following levels of Yb are located: $4f^{13}\,6s^2 6p$ $(7/2,\ 3/2)_5$ (35 178.78 cm^{-1}), $4f^{13}\,6s^2 6p$ $(7/2,\ 3/2)_2$ (35 196.98 cm^{-1}, $4f^{13}\,6s^2 6p$ $(7/2,\ 3/2)_3$ (35 807.52 cm^{-1}), and $4f^{13}\,6s^2 6p$ $(7/2,\ 3/2)_4$ (36 090.98 cm^{-1}). Again, the selection rules give the only level, namely, $4f^{13}\,6s^2 6p$ $(7/2,\ 3/2)_2$. The HFS and isotopic shifts of the $^3P_1 \rightarrow (7/2,\ 3/2)_2$ transition frequency prove to be sufficiently large to provide the high excitation selectivity for almost any of the ytterbium isotopes, in particular, ^{168}Yb (Table 2).

Table 2. Parameters of the $(7/2,3/2)_2 \rightarrow 6\,^3P_1$ transitions taking into account the isotopic and hyperfine structures of Yb isotopes (experimental data [4]; the error is ~ 10 MHz).

A	$F' - F$	$\Delta\nu$/MHz
168	**2–1**	**−10293**
171	3/2–3/2	−8805
170	2–1	−6318
171	5/2–3/2	−5973
173	1/2 - 3/2	−4147
173	3/2–3/2	−3612
173	5/2–3/2	−3302
171	3/2–1/2	−2862
172	2–1	−2711
173	7/2–5/2	−2532
173	3/2–5/2	−2126
173	5/2–5/2	−1833
173	9/2–7/2	−732
174	2–1	0
173	7/2–7/2	2172
176	2–1	2578
173	5/2–7/2	2894

Note: The ^{168}Yb isotope of most practical interest is presented in bold.

Note that, when other dyes are used, the $4f^{14}6s7s\,^1S_0$ level (34 350.65 cm^{-1}) can be also used as the third level in the photoionisation scheme; however, the isotopic structure of this level is less convenient for separating the ^{168}Yb isotope than that of the $4f^{13}\,6s^2 6p$ $(7/2,\ 3/2)_2$ level [4].

Autoionisation states. The fourth level (AIS) of the scheme should have the energy in the range from 51 790 to 53 720 cm^{-1} or should be exactly equal to 54 784 or 52 492 cm^{-1} (if we use directly radiation from a copper vapour laser). This level should be odd and should have the total momentum $J = 1$, 2, or 3.

The authors of papers [4] found four AISs to which the transition can occur from the third $[7/2,3/2]_2$ level of the selective photoionisation scheme. The intense transitions to AISs with energies 52 353 and 52 609 cm^{-1} were observed. The cross section for the transition to the 52 353-cm^{-1} AIS was measured and the photoionisation spectra covering the AISs with energies 52 353 and 52 609 cm^{-1} were obtained. From these spectra, the cross section for the 52 609-cm^{-1} transition can be also estimated (Fig. 3). The ionisation cross section for the 52 353-cm^{-1} transition is $\sigma_i = (6 - 7) \times 10^{-16}$ cm^2 (for $\lambda = 582.79$ nm resonant with the AIS peak). The cross section for ionisation by the 581.067-nm laser line resonant with the 52 609 cm^{-1} transition is approximately lower by a factor of seventeen and is $(3 - 4) \times 10^{-17}$ cm^2.

It is interesting to use the $[7/2,3/2]_2 \rightarrow 5d6p\,^3D_1$ transition (51 797 cm^{-1}, 601.9 nm) for photoionisation. In this case, the dye can be pumped both by the green and yellow lines of a copper vapour laser. However, according to [4],

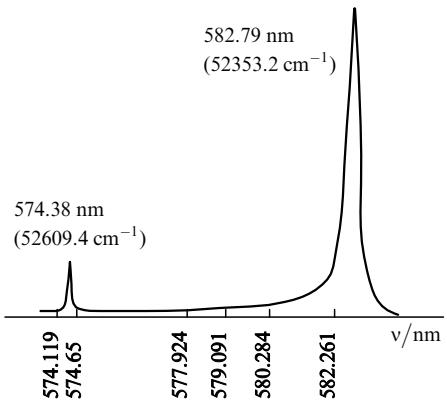

Figure 3. Part of the spectrum of photoionisation from the $[7/2,\ 3/2]_2$ level [4].

the 51 797-cm^{-1} transition and other transitions are weak because they were not observed in the photoionisation spectrum. This means most likely that the cross section for these transitions are lower than that for the 52 353-cm^{-1} transition by a factor of 50 and more.

The measurements of the ground-state absorption spectra of ytterbium [43, 44] give no information on the cross section for photoionisation from the excited $[7/2,3/2]_2$ state because two different two-electron transitions couple the ground state and the third working level with the AIS in the photoionisation scheme. However, knowing the cross section for the first of these transitions, we cannot estimate the cross section for the second one. It only follows from general considerations that the second transition should be greatly complicated compared to the first one. In addition, the probability of the second transition should be substantially lower due to the lower energy gap.

The search for AISs initiated in Ref. [4] was continued in Ref. [45], where, however, the cross section for the 601.9-nm transition was also not determined (Figs 4, 5). Although the corresponding spectra were recorded, they cannot be 'joined' in order to estimate the cross section because the scale over the y axis and the position of zeroes on this axis are not presented. According to Ref. [45], the 51 797-cm^{-1} transition has a moderate intensity, while the 52 353-cm^{-1} transition is strong. Note that, according to Ref. [45], the 52 606-cm^{-1} transition is approximately ten times more

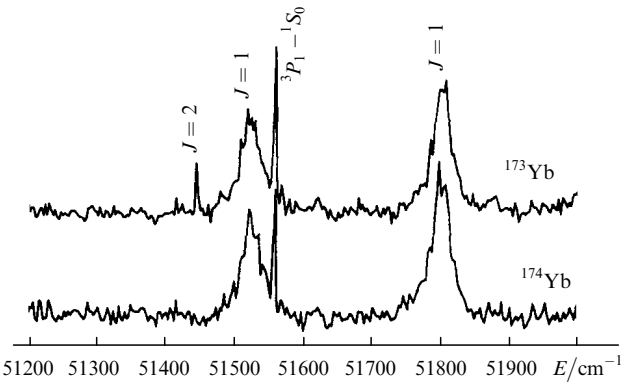

Figure 4. Part of the spectrum of photoionisation from the $[7/2,\ 3/2]_2$ level [45].

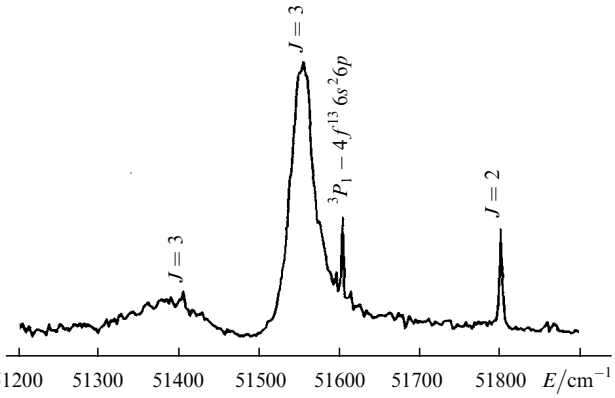

Figure 5. Same as in Fig. 4 for the spectral region containing the resonance recommended in Ref. [4].

intense than according to Ref. [4], which seems to be correct. This explained by the fact that $J = 2$ for the corresponding AIS (which was found in Ref. [45]). However, this transition is forbidden for polarisations of laser radiation used in Ref. [4]. In addition, the authors of paper [45] found several 'longer-wavelength' AISs, the transition to one of them being estimated as strong (the absolute value of the cross section is also unknown).

The parameters of some AISs found in Ref. [45], which can be used as the fourth level in the photoionisation scheme, are listed together with the AIS parameters from paper [4] in Table 3.

According to the data presented above, scheme (1) is optimal at present. Note, however, that the AIS spectrum is studied insufficiently. It is possible that new AISs will be found, and the scheme for selective photoionisation at the third step can be improved.

Formulation of the problem and the method for its solution. We considered the problem of photoionisation of an optically thin layer of Yb vapours with the natural isotopic composition by radiation from three spatially combined linearly polarised laser beams (see also [18]). The first laser was tuned to the $^1S_0 - ^3P_1$ transition ($\lambda_{12} = 555.648$ nm), the second one – to the $^3P_1$ – $(7/2, 3/2)_2$ transition ($\lambda_{23} = 581.067$ nm), and the third one – to the $(7/2,3/2)_2$-AIS transition.

The temporal shape of the laser pulses was assumed trapezoidal (the durations of the leading and trailing edges of pulses and of their flat tops were specified). Also, the delays of pulses from each of the lasers with respect to the zero time were specified independently. The typical FWHM duration of the laser pulse was 20 ns, delays between the pulses were varied between 0 and 80 ns. The pulse intensity was usually adjusted to provide the average power of the beam of cross section 1 cm^2 in the repetitively pulsed regime equal to ~ 1 W.

The emission lines of the first and second lasers were described by Gaussians or Lorentzians (the linewidth and shape were specified for each of the lasers). The shape of the emission line from the ionising laser is insignificant because of a large width of the AIS level.

The medium (Yb vapours) was characterised by the density and distribution of atoms over the velocity projections on the direction of propagation of laser beams. The atoms in the medium were divided into $n = 5 - 15$ groups over the velocity projections. For each of the velocity groups, the rate equations were recorded for a total system of HFS sublevels of the first, second, and third levels and the AIS for each of the Yb isotopes (altogether $50n$ equations were solved). The velocity distribution of atoms could be specified arbitrarily (we used the Maxwell distribution in our calculations).

The system of rate equations was solved by the standard fourth-order Runge–Kutta method. A typical time step was 0.05–0.5 ns. The ionisation kinetics was calculated using a PC 486/66 (the process duration is ~ 150 ns) for the specified laser wavelengths during 20–40 s.

Rates of processes and the kinetic model. We considered the following processes:

(i) excitation (deexcitation) by laser radiation and spontaneous radiative decay of levels 1, 2, and 3;

(ii) photoionisation (via the AIS) by the second and third lasers from the level 3. Ionisation by the second laser should be taken into account because of a large width of the AIS: the transition from the level 3 to the continuum at the wavelength of the second laser falls on the AIS wing and has a noticeable intensity;

(iii) the radiative decay of the level 3 to the states ignored in the model.

The rate of the stimulated optical transition in an atom with the velocity projection v on the direction of propagation of the laser beam, when the laser linewidth is much greater than the natural linewidth of the atom and the field broadening of the levels can be neglected (the field linewidth is much smaller than the width of the velocity distribution of atoms), can be written in a simple form

$$K(v,t) = \frac{\lambda^2}{4} A \frac{I_{\text{las}}(t) S_{\text{las}}[\omega_0(1 + v/c)]}{\hbar\omega} = \sigma_{\text{ph}} \frac{I}{\hbar\omega}.$$

Here, S_{las} is the laser spectrum; $\int S_{\text{las}}(\omega)\mathrm{d}\omega = 1$; I_{las} is the laser radiation intensity; ω_0 is the atomic-transition

Table 3. Parameters of the AIS that can be used as the fourth level in the photoionisation scheme for ytterbium [4, 45] (data [45] are presented in parentheses).

The $[7/2, 3/2]_2 \rightarrow$AIS transition wavelength/nm	AIS energy/cm^{-1}	Transition linewidth/cm^{-1}	Transition cross section/cm^{-2}	Total momentum J
574.38*	52609.4 (52601.8)	1.5 (2.91)	$2 \times 10^{-17}(2 \times 10^{-16})$	2
582.79*	52353.2 (52349.9)	13.5 (14.5)	6.7×10^{-16}	3
588.75*	52186.0 (52187.2)	77 (106)	–	3
601.91*	51797.0 (51805.2)	25 (35)	–	1
(615.7**)	(51439.2)	(2)	–	2
(612.6**)	(51520.1)	(50)	–	1
(602.1**)	(51805.2)	(35)	–	1

* measured in air, ** measured in vacuum.

frequency: A is the atomic-transition probability; and σ_{ph} is the transition cross section.

The probabilities of the $1 \to 2$ and $2 \to 3$ transitions are

$$A_{12} = 3.6 \times 10^6 Q(0IFM, 1IF'M', \mu),$$

$$A_{23} = 1.9 \times 10^5 Q(1IFM, 2IF'M', \mu),$$

where

$$Q(JIFM, J'IF'M', \mu) = (2F+1)(2F'+1)$$

$$\times \begin{pmatrix} F & 1 & F' \\ -M & \mu & M' \end{pmatrix}^2 \begin{Bmatrix} J & F & I \\ F' & J' & 1 \end{Bmatrix}$$

is the angular factor for transitions between the HFS components; $(\cdots)$ are the $3jm$ Wigner symbols; $\{\cdots\}$ are the $6j$ symbols; F is the total angular momentum of the atom; J, I are the momenta of the atomic level and nucleus, respectively; M is the total momentum projection; μ is polarisation ($\mu = 0$ for linear polarisation and $\mu = \pm 1$ for circular polarisation; we used plane polarised light). The photoionisation cross section is described by the expression

$$\sigma_{ph} = 7.8 \times 10^{-15} \sum_F Q(2IFM, 3IF'M', \mu).$$

The broadening of atomic lines under conditions considered here is mainly determined by the Doppler effect. For the Maxwell distribution of atoms over velocities, the spectral function is described by the known expression

$$S_D(\Delta\omega) = \frac{1}{\sqrt{\pi}\Delta\omega_D} \exp[-(\Delta\omega/\Delta\omega_D)^2],$$

$$\Delta\omega_D = \omega_0 v_T/c, \quad \Delta\omega = \omega - \omega_0,$$

where ω_0 is the frequency of the atomic transition; $v_T = (2T/M_{Yb})^{1/2} \approx 1.1 \times 10^5 \sqrt{T}$ is the thermal velocity of atoms ($M_{Yb} \approx 173 \times 1.67 \times 10^{-24}$ g; and T is the vapour temperature). We assume for estimates that $T \approx 0.1$ eV and $\lambda \approx 580$ nm. Then, we obtain $vT \approx 3.4 \times 10^4$ cm s^{-1} and, correspondingly, $\Delta\omega_D \approx 3.6 \times 10^9$ c^{-1}, and $\Delta\nu_D \approx 570$ MHz.

The relaxation rate of the sublevels of the level 3 is the same due to the orthogonality and completeness of the $3jm$ symbols (is independent of $JIFM$). Generally speaking, this dependence appears if we exclude from the expression for the decay rate the channels taken into account in the model. However, because the relaxation rate is mainly determined by the transitions to the states neglected in the model, this dependence can be ignored.

The angular factors determine the selection rules over the momentum projection. Note that the selection rules for laser and natural (nonpolarised) radiations are different: $M = M'$ for linearly polarised radiation, $M = M' \pm 1$ for circular polarisation, and $|M' - M| = M \leqslant 1$ for spontaneous radiation. For this reason, the probabilities of the laser and spontaneous transitions are, generally speaking, different: the statistical weight of the lower level of a laser is equal to that of the upper level, whereas statistical weights for spontaneous transitions are proportional to momenta.

We assume in our model that laser radiation is linearly polarised. Because the total momenta of the chains of levels for even ^{171}Yb isotopes do not decrease, there is no need to separate individual magnetic sublevels in the kinetic model and its sufficient only to calculate the probabilities of laser transitions. For ^{173}Yb, individual magnetic sublevels should be separated. To reduce the number of levels taken into account, we combined the sublevels with equal absolute values of M and recalculated appropriately the probabilities. Note that such a combination of sublevels can be performed only when laser radiation is linearly polarised. In the case of circular or elliptic polarisation, all the levels should be considered separately.

Our calculations showed that the high selectivity and efficiency of ionisation of ^{168}Yb can be provided if the emission wavelength of the laser inducing the second transition is equal to 581.0785 ± 0.0005 nm.

Note that the laser line has long wings, which can be caused by various factors (see details in Ref. [18]). Because the initial content of the required isotope is very small, emission in these wings can substantially deteriorate the ionisation selectivity. We simulated long tails in our calculations by placing the laser line on a 'pedestal' of height S, which was specified by three points based on some considerations.

Our calculations showed (Fig. 6) that, if the laser-line wing extends to the long-wavelength region by 0.007 nm (6 GHz), then its influence on the isotopic composition becomes substantial already at the spectral energy contrast of ~ 100. The spectral energy contrast is the ratio of the spectral energy density emitted by the laser at the line centre to the maximum spectral density emitted by this laser in the wings for detuning $|\Delta\nu| > 1.5$ GHz. The frequency 1.5 GHz corresponds to the detuning of the energy level of a nearest isotope from the frequency of the second-step laser.

2.2 Production of a highly enriched isotope

Basic parameters. By omitting details, we give the basic parameters that were used in calculations to optimise different units of the setup [14–19]. These are the vapour density in the ionisation region, which was $(1-5)\times$

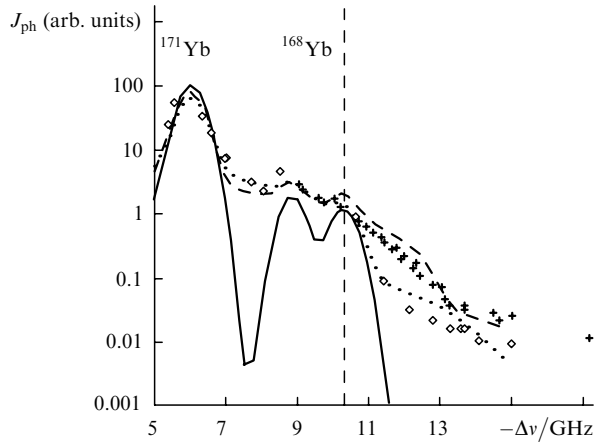

Figure 6. Dependence of the photocurrent J_{ph} on the detuning $\Delta\nu$ of the laser exciting the second (selecting $4f^{14}6s6p\,^3P_1 \to 4f^{13}6s^26p\ (7/2,3/2)_2$ transition ($\Delta\nu$ is measured with respect to the frequency of this transition in the ^{174}Yb isotope). The solid curve is calculated for $s = 0$ for laser radiation (points in the curve are calculated at intervals of 250 MHz), squares and crosses are results obtained in two series of experiments performed under different conditions. The dashed curve corresponds to a pedestal at which the calculations well agree with experimental results presented by crosses ($s = 0.02$ for the frequency detuning $\Delta\nu' = \pm 5$ GHz and $s = 0.05$ for $\Delta\nu' = 0$); the maximum content of ^{168}Yb is 51 %. The dotted curve corresponds to squares ($s = 0.002$ for $\Delta\nu' = \pm 7$ GHz, $s = 0.02$ for $\Delta\nu' = 0$); the maximum content of ^{168}Yb is 54 %.

10^{12} cm^{-3} for the ionisation-region length of 1 m and its cross section of 5–10 cm^2, as well as the average powers of dye lasers, which were $\sim$ 1 W at 555.6 and 581.1 nm and 3–5 W at 582.8 nm for a pulse repetition rate of 10 kHz. These parameters determine to a great extent the design of the setup, whose principal scheme is shown in Fig. 7.

System of copper vapour lasers and dye lasers. Dye lasers were pumped by LM-8, LM-25, and LM-50 copper vapour lasers developed at Istok State Research and Production Association [46]. The FWHM duration of the laser pulse was 15 ns and the pulse repetition rate was 10 kHz. The LM-8 laser was used as a master oscillator, while the other lasers were used as amplifiers. Stabilised power supplies and a system of LC peaking circuits provided the high temporal and amplitude stability of output laser pulses, and an electronic multichannel unit synchronised laser pulses with an accuracy of 1–2 ns. The average output power at 510 nm was 18 and 30 W when the LM-25 and LM-50 amplifiers, respectively, were used. The system of dye lasers also consisted of three channels, each of them containing a master oscillator and an amplifier. The output power of the third channel providing photoionisation was enhanced with the help of the second amplifier (LM-50). We used lasers described in [47, 48].

The emission line was formed in the master oscillator in which a diffraction grating and a Fabry–Perot etalon were used as selecting elements. The laser wavelength was measured with a wavelength meter, which was calibrated using a stabilised He–Ne laser. In addition, the quality of laser radiation was controlled by the ion composition of the laser plasma measured with a mass spectrometer. The radiation formed with the help of master oscillators was then amplified with amplifiers whose efficiency amounted to 25 %.

We used two dyes, R6G and R110. The efficiency of the master oscillator was 20 %–25 % without etalon and 15 %–18 % with etalon. The half-widths of the laser lines at the first and second excitation steps, measured with a Fizeau interferometer and a scanning Kahn interferometer, did not exceed 0.5 GHz (see section 2.3).

The short-term laser wavelength instability was $\sim$ 200 MHz, while the long-term instability, determined by temperature variations, was 400 MHz h^{-1}. During a long operation (up to 16 h of continuous operation), the spectral and energy parameters of lasers were well reproduced. The temperature drift of the laser frequency was corrected at intervals of 0.5 h.

In late 1997 a larger laser setup was constructed with the active length of a vacuum chamber equal to 4.5 m. The output power of copper vapour lasers and dye lasers was enhanced. In all the cases, a three-stage amplification was used.

Equipment inside the chamber. The equipment placed inside the vacuum chamber included an evaporator, a system of extractors, vapour-density sensors, and a mass spectrometer. A Joule's heat evaporator was used which consumed power up to 3 kW and produced atomic vapours of density up to 10^{13} cm^{-3} for many hours in the ionisation region. The atomic beam was formed in a number of experiments with the help of elongated tubes or similar guiding elements. The evaporator demonstrated during prolonged operation a high reliability, the absence of the slit overgrowing and good reproducibility of the atomic beam parameters. The degree of isotope enrichment was measured with a constant-magnet mass spectrometer equipped with a PC.

Experimental results. Using the setup described above, we performed many experimental studies on the formation of vapour flows, the dependence of the ionic composition of the current on the wavelength, shape, and power of laser lines at different excitation steps, as well as on the configuration of the region irradiated by lasers.

The main experiments were performed under the following conditions: the width of laser lines at the first and second steps was $\sim$ 500 MHz; the output powers of lasers at the first, second, and third excitation (ionisation) steps were 1, 1, and 4 W, respectively; the vapour density in the ionisation region was $10^{11}-10^{13}$ cm^{-3}; the cross section of the ionisation zone was 1–4 cm^2, and the working voltages applied to extractors were 100–3800 V.

In 1996–1997, ion currents of 0.5–1.5 mA per 1 m of the active medium were achieved on the setup collector, corresponding to the production of 3–10 mg h^{-1} of

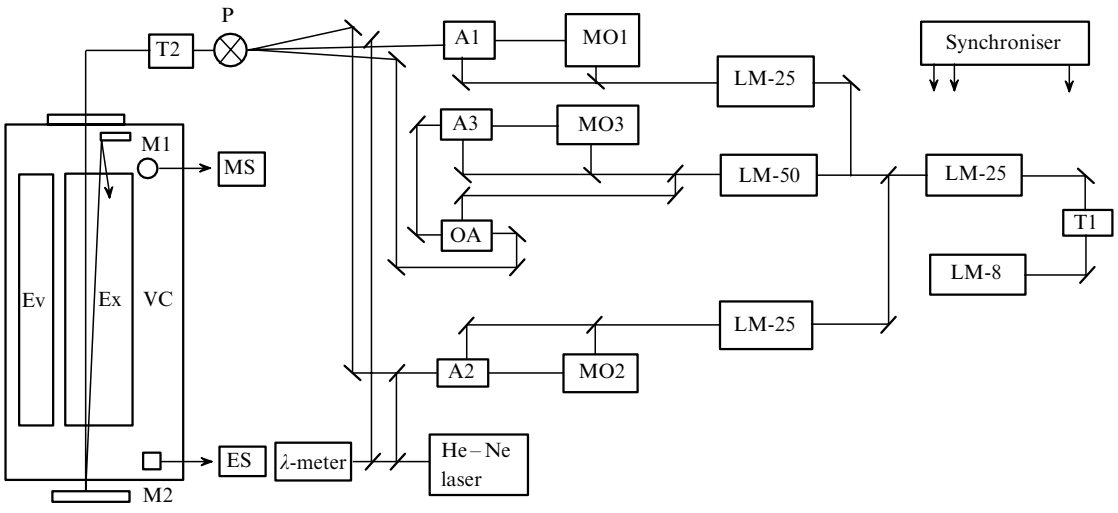

Figure 7. Scheme of the setup [1, 2] for laser separation of ytterbium in weighable amounts: LM-8: copper vapour master oscillator; LM-25, LM-50: copper vapour amplifiers; T1: beam expander; MO: dye master oscillator; A: dye amplifier; OA: output dye amplifier; P: periscope; T2: telescope; M1, M2: mirrors; Ev: evaporator; Ex: extractor; MS: mass spectrometer; FS: flux sensor; VC: vacuum chamber.

enriched ytterbium from 1 m of the active medium. During a month the setup operated for more than 200 hours, producing 0.5–1 g of the enriched isotope. According to the independent mass-spectrometric analysis performed at GIREDMET, the content of ^{168}Yb in the material deposited on the collector was increased up to 62 %. The content of ^{168}Yb in the wash solution was 45 %.

The results presented above demonstrate that the LIS problem was developed to a qualitatively higher level. Because the cost of highly enriched (no less than 25 %) ^{168}Yb is high, it is profitable to produce even 1 g of ^{168}Yb per month. Therefore, commercially profitable production of the enriched isotope was performed for the first time in the world.

3. Laser separation of palladium isotopes

3.1 Scheme for two-step ionisation of palladium

Schemes of selective ionisation. Transitions from the ground state of palladium to its excited states lie in the UV spectral region. If dye lasers pumped by copper vapour laser are used, the $4d^{10}\,{}^1S_0 - 4d^9\,5p\,{}^3P_1$ transition in palladium at 276.4 nm can be used as the first transition in the photoionisation scheme. This transition was used in papers [36, 37], where the attempt of enrichment of ^{105}Pd using two-step ionisation by one laser was made.

Several possible schemes of step ionisation were considered (Fig. 8).

(1) The first group of schemes is based on two-step or three-step photoionisation of palladium atoms via the $4d^9\,5p\,{}^3P_1$ state. The first transition $4d^{10}\,{}^1S_0 - 4d^9\,5p\,{}^3P_1$ in the scheme is excited at 276.4 nm and is a selecting one. Then, in the case of the two-step ionisation, atoms are either directly ionised to continuum by UV radiation below 322 nm or are ionised via autoionisation Rydberg states $4d^9np$, and $4d^9nf$. In the case of three-step ionisation, one of the higher electronic states is excited (for example, $4d^9\,5p$). Photoionisation from these states can be performed directly by a copper laser.

(2) The second group of schemes is based on the accumulation of atoms in the $4d^9 5p\,{}^3P_1$ metastable states. The first transition, as in the first group of schemes, is excited at 276.4 nm. The excited $4d^9 5p\,{}^3P_1$ state undergoes a spontaneous decay to the states $4d^9 5s\,{}^1D_2$ and $4d^9 5s\,{}^3D_2$. Then, one of the transitions to the $4d^8 5s5p$ states can be used for selection. The wavelengths of these transitions are 255.1 nm ($^1D_2 \rightarrow E = 50910$ cm^{-1}), 245.4 nm ($^1D_2 \rightarrow E = 52457$ cm^{-1}), 231.7 nm ($^3D_2 \rightarrow E = 50910$ cm^{-1}), and 223.6 nm ($^3D_2 \rightarrow E = 52457$ cm^{-1}). Ionisation from the states with energies 50 910.4 cm^{-1} ($J = 3$) and 52 457.0 cm^{-1} ($J = 3$) is performed either via the autoionisation Rydberg states $4d^9np$, $4d^9nf$ by copper vapour laser-pumped tunable dye lasers or directly by the lines from a copper vapour laser.

These schemes were considered in papers [38–40]. We present the results of new calculations based on the recent data [40].

The use of the Zeeman effect. The blending of isotope lines appearing due to the hyperfine splitting of the lines of isotopes with nonzero nuclear momenta often prevents the achievement of a high selectivity of photoionisation of a rare isotope. In these cases, in particular, to separate ^{102}Pd it was proposed [39] to use the Zeeman effect to shift blending lines outside the laser linewidth and the Doppler width of the atomic lines.

To calculate the Zeeman effect for obtaining the energies of the sublevels of a level with the momentum J and determining the transition probabilities in an external static magnetic field, it is necessary to diagonalise the matrix of perturbation of an atom by the magnetic field $W_{i,j} = \langle JF_iM_i|V|JF_jM_j\rangle + \delta_{ij}\varepsilon_i$, which is constructed on the basis of unperturbed wave functions. Here, $V = g_j\mu_B B\hat{J}$ is the perturbation operator (g_J is the gyromagnetic ratio, or the g factor, $g_{^3P_1} = 1.396$); μ_B is the Bohr magneton; B is the magnetic field strength; $\hat{J}$ is the electronic-shell momentum operator; $F = J + I$ is the total momentum of the HFS sublevel (I is the nuclear moment); the subscripts i and j number the HFS sublevels of the J level (with total momenta F_i and projections M_i); and ε_i is the energy of

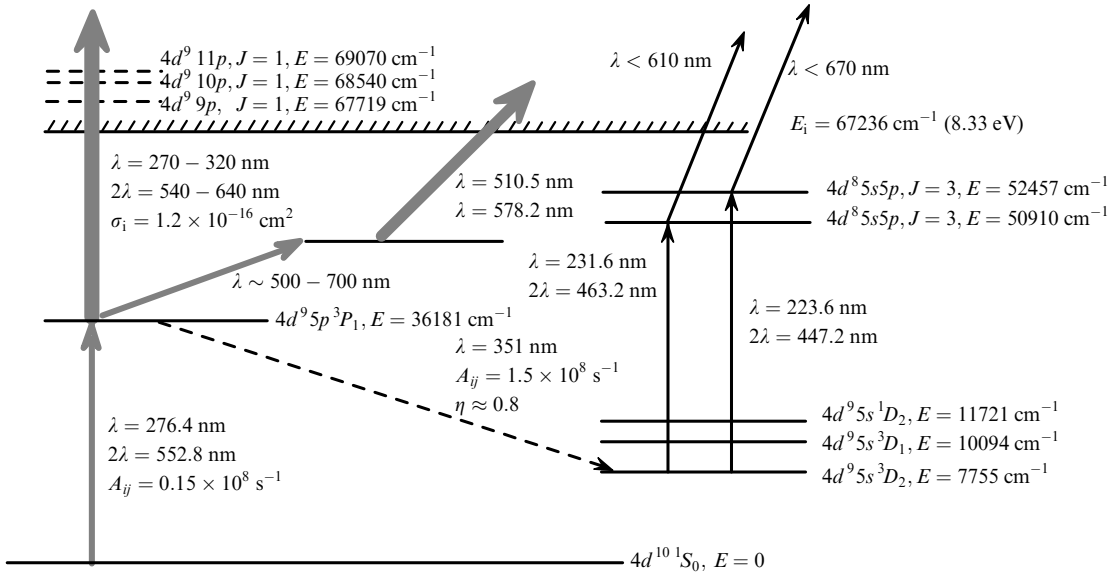

Figure 8. Schemes for Pd photoionisation (E_i is the ionisation energy).

the ith level of the HFS in the absence of a magnetic field.

Analysis of the calculations shows that, when the magnetic field strength (induction) exceeds 1500 G, the lines corresponding to transitions to the magnetic sublevels in ^{105}Pd, which most strongly prevent the selective ionisation of ^{102}Pd, are shifted at least by 1000 MHz from the working transition frequency, which can provide the selective ionisation of ^{102}Pd.

Note that to perform efficient excitation of atomic levels in a magnetic field, the vector of the electric field strength in a laser beam should be parallel to the magnetic field vector, while the laser beam should be perpendicular to the vector ***B***.

Calculations of the spectral dependence of the photocurrent and ionisation efficiency. To calculate the dependences of the photocurrent spectrum on the laser wavelength exciting the $4d^{10}\,{}^1S_0 \rightarrow 4d^9 5p\,{}^3P_1$ transition and on the magnetic field strength, the multilevel kinetic photoionisation model was developed, which is similar to that used for the description of ytterbium ionisation. This model takes into account the simultaneous ionisation of all the isotopes excited by a laser and allows one to determine the isotope enrichment achieved upon selective photoionisation.

The problem of photoionisation of an optically thin Pd vapour layer was considered. The natural isotopic composition of Pd vapours was assumed. The laser line was described by a Gaussian or a Lorentzian (the linewidth and shape were specified). The laser line shape is insignificant both upon ionisation to continuum and ionisation via the AIS (because of a large width of the latter).

The problem was solved in two stages. At the first stage, the Zeeman magnetic sublevels of the $4d^9 5p\,{}^3P_1$ level were determined for all the palladium isotopes in a specified magnetic field and the probabilities of allowed transitions between them were calculated. The probabilities of radiative transitions and the structure of the $4d^9 5p\,{}^3P_1 \rightarrow 4d^{10}\,{}^1S_0$ transition [42] are presented in Tables 4–6.

Table 4. Transition probabilities for even Pd isotopes calculated from the data [42].

Transition	A_{ij}/s^{-1}
$4d^9 5p\,{}^3P_1 \rightarrow 4d^{10}\,{}^1S_0$	1.5×10^7
$4d^9 5p\,{}^3P_1 \rightarrow 4d^9 5s\,{}^3D_2$	1.5×10^8
$4d^9 5p\,{}^3P_1 \rightarrow 4d^9 5s\,{}^3D_1$	2.1×10^7
$4d^9 5p\,{}^3P_1 \rightarrow 4d^9 5s\,{}^1D_2$	4.3×10^6

The medium (Pd vapours) was described by the density and distribution of atoms over the velocity projections on the direction of propagation of laser beams (atoms in the medium were divided into $n = 5 - 15$ groups). For each velocity group, the rate equations (in the intensity approximation) were written for a total system of all the sublevels of the $4d^9 5p\,{}^3P_1$ level for each of the Pd isotopes. The velocity distribution of atoms could be specified arbitrarily; below, the Maxwell (Gaussian) distribution was used. The system of rate equations was solved by the standard fourth-order Runge–Kutta method.

The system of rate equations described the following processes: laser excitation (deexcitation) of the $^3P_1$ level, the radiative decay of this level to the states neglected in the given model, and photoionisation to a continuum by exciting and ionising lasers (with the cross section $\sigma_i = 1.2 \times 10^{-16}$ cm^2). Note that the relaxation rate of all the sublevels of the $^3P_1$ level is the same (independent of *JIFM*) due to the orthogonality and completeness of the 3*jm* symbols.

Table 5. Probabilities of transitions between the HFS sublevels in ^{105}Pd calculated from the data [42].

Transition	A_{ij}/s^{-1}
$4d^9 5p\,{}^3P_1\ F = 3/2 \rightarrow 4d^{10}\,{}^1S_0\ F = 5/2$	1.5×10^7
$4d^9 5p\,{}^3P_1\ F = 5/2 \rightarrow 4d^{10}\,{}^1S_0\ F = 5/2$	1.5×10^7
$4d^9 5p\,{}^3P_1\ F = 7/2 \rightarrow 4d^{10}\,{}^1S_0\ F = 5/2$	1.5×10^7
$4d^9 5p\,{}^3P_1\ F = 3/2 \rightarrow 4d^9 5s\,{}^3D_2\ F = 1/2$	4.6×10^7
$4d^9 5p\,{}^3P_1\ F = 3/2 \rightarrow 4d^9 5s\,{}^3D_2\ F = 3/2$	6.4×10^7
$4d^9 5p\,{}^3P_1\ F = 3/2 \rightarrow 4d^9 5s\,{}^3D_2\ F = 5/2$	4.3×10^7
$4d^9 5p\,{}^3P_1\ F = 5/2 \rightarrow 4d^9 5s\,{}^3D_2\ F = 3/2$	1.8×10^7
$4d^9 5p\,{}^3P_1\ F = 5/2 \rightarrow 4d^9 5s\,{}^3D_2\ F = 5/2$	5.6×10^7
$4d^9 5p\,{}^3P_1\ F = 5/2 \rightarrow 4d^9 5s\,{}^3D_2\ F = 7/2$	7.9×10^7
$4d^9 5p\,{}^3P_1\ F = 7/2 \rightarrow 4d^9 5s\,{}^3D_2\ F = 5/2$	5.5×10^6
$4d^9 5p\,{}^3P_1\ F = 7/2 \rightarrow 4d^9 5s\,{}^3D_2\ F = 7/2$	3.3×10^7
$4d^9 5p\,{}^3P_1\ F = 7/2 \rightarrow 4d^9 5s\,{}^3D_2\ F = 9/2$	1.1×10^8

Table 6. Hyperfine and isotopic structures of the $4d^9 5p\,{}^3P_1 \rightarrow 4d^{10}\,{}^1S_0$ transition [42].

A	F	$\Delta\nu$/MHz
105	3/2	446
105	5/2	125
102	1	125
104	1	55
^{105}Pd*	–	0
106	1	−18
108	1	−81
110	1	−147
105	7/2	−317

* centre of gravity of the HFS of ^{105}Pd.

The polarisation of laser radiation was described by a mixture of linear polarisation with left-hand and right-hand circular polarisations, the fraction of each of them being specified.

The calculations show (Fig. 9) that in the absence of a magnetic field the required enrichment of the ^{102}Pd isotope cannot be achieved due to the overlap of its line with the line of the ^{105}Pd isotope. In a magnetic field of 2000 G, the required enrichment is achieved (at the acceptable ionisation efficiency) within a comparatively narrow tuning range of a selecting laser (0–60 MHz).

3.2 Experimental results

Photoionisation cross section. The dependence of the two-step ionisation efficiency (involving the $4d^{10}\,{}^1S_0 \rightarrow 4d^9 5p\,{}^3P_1$, $\lambda = 276.4$ transition at 276.4 nm) on the laser radiation intensity was measured in paper [39]. It was shown that the efficient (above 50 %) two-step ionisation of palladium by 10-ns laser pulses with a pulse repetition rate of 10 kHz can be achieved when the average laser radiation intensity exceeds 100 W cm^{-2}. A comparison of calculations with the measurements of the efficiency of two-step ionisation gives the estimate $\sigma_i \approx 10^{-16}$ cm^2 of the ionisation cross section for the $4d^9 5p\,{}^3P_1$ state. Note that these results do not agree with the results obtained in Ref. [36]. The required laser radiation intensity determined in experiments [39] is an order of magnitude greater than that obtained in Ref. [36]. Correspondingly, the photoionisation

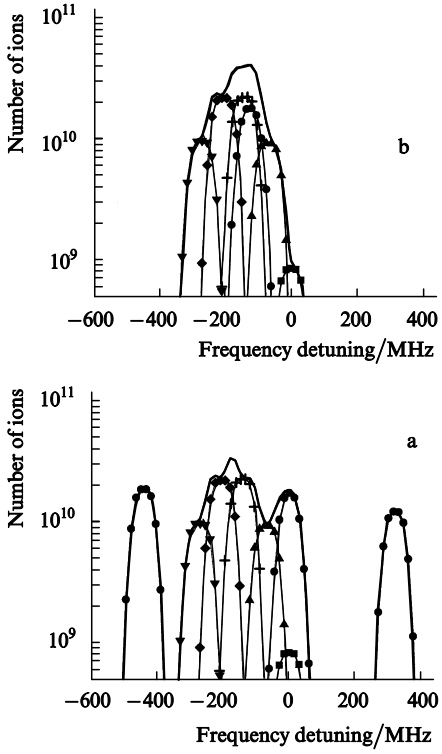

Figure 9. Dependences of the isotopic composition of ions on the detuning of the first (selecting) laser in the absence of a magnetic field (a) and in a magnetic field of 2000 G (b) for the peak pulse intensities of the first and second lasers of 500 W cm^{-2} and 50 kW cm^{-2}. The detuning is measured with respect to the transition frequency in ^{102}Pd, the width of atomic lines and the laser line are assumed equal to 30 MHz, polarisation of radiation is assumed linear. The solid curve is the total number of ions produced in the ionisation region per pulse; the curves with symbols are the numbers of palladium isotopes with the mass numbers equal to 102 (■), 104 (▲), 105 (●), 106 (+), 108 (◆), and 110 (▼).

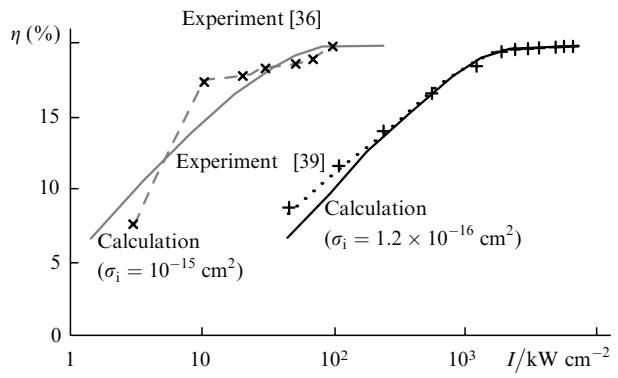

Figure 10. Dependence of the efficiency of two-step ionisation of palladium on the laser pulse intensity.

cross section $\sigma_i \approx 10^{-15}$ cm^2 measured in experiments [36] is also an order of magnitude greater. Such a cross section is usually observed near autoionisation states. Because there is no autoionisation states in the region of continuum under study, experimental results [39] seem to be more reliable.

Mass spectra of enriched isotopes. The dependences of mass spectra of palladium on the laser frequency at the first excitation step were studied in paper [40]. Typical mass spectrograms for predominantly enriched ^{104}Pd and ^{105}Pd,

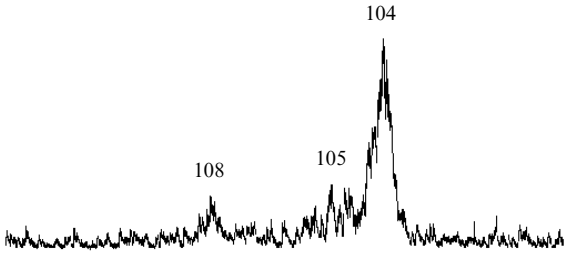

Figure 11. Typical mass spectrogram with the predominantly enriched ^{104}Pd isotope in the absence of a magnetic field. Here and in Figs 12 and 13, the mass numbers of isotopes are indicated at the spectral peaks. The content of ^{104}Pd is 67 %.

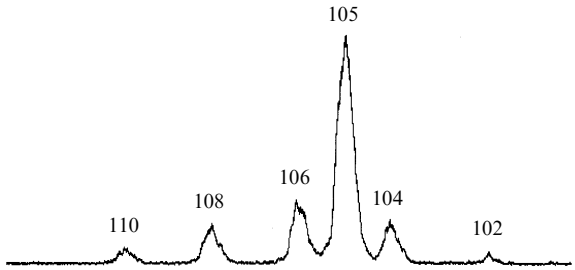

Figure 12. Typical mass spectrogram with the predominantly enriched ^{105}Pd isotope in the absence of a magnetic field. The content of ^{105}Pd is 60 %.

obtained in the absence of a magnetic field, are shown in Figs 11 and 12. The maximum content of the ^{102}Pd isotope in the mass spectra achieved in our experiments in the absence of a magnetic field did not exceed 3 %–4 %.

The content of the ^{102}Pd isotope among the ions obtained upon photoionisation drastically increased when a magnetic field was used in the region of selective photoionisation. In experiments on the ^{102}Pd isotope separation, the first-step laser frequency was tuned to achieve the maximum ^{102}Pd isotope enrichment. The linear polarisation of radiation from the first-step laser in the photoionisation region was collinear to the magnetic field strength. The average value of the magnetic field strength in the region of selective photoionisation estimated from the Zeeman shifts of transition frequencies in ^{105}Pd was 2.4 ± 0.5 kG. The typical mass spectrogram obtained upon separation of ^{102}Pd in a magnetic field is shown in Fig. 13.

The content of the ^{102}Pd isotope in mass spectra in experiments on the separation of ^{102}Pd in a magnetic field varied from 10 % to 18 % (compared to the natural content of 1 %). In addition, other isotopes were substantially

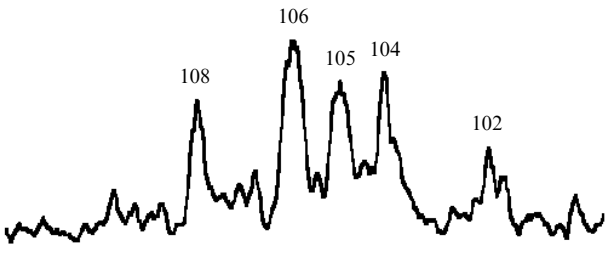

Figure 13. Typical mass spectrogram with the predominantly enriched ^{102}Pd isotope obtained in a magnetic field of 2400 G.

enriched (Figs 11 and 12): ^{104}Pd – up to 70 % (the natural content being 11.4 %) and ^{105}Pd – up to 60 % (22.33 %).

Measurements [40] of the isotopic spectra upon scanning the excitation line of the $4d^{10}\,{}^1S_0 \rightarrow 4d^9 5p\,{}^3P_1$ transition are in qualitative agreement with the results of calculations presented above, which were based on spectroscopic data presented in paper [42], and do not agree with the data reported in [36]. We believe that the data [42] are much more reliable.

4. Conclusions

Let us summarise the basic results on the separation of rare isotopes.

(i) We have managed to solve the key problems of laser separation of the weighable amounts of the ^{168}Yb isotope with an initial low content in the natural mixture. The cost of the highly enriched (above 25 %) ^{168}Yb is high because of its very low content in the natural mixture. For this reason, it is profitable to produce even 1 g of ^{168}Pd per month. Therefore, we have achieved commercially efficient production of the enriched isotope by the LIS method for the first time in the world.

(ii) Using selective two-step ionisation, we have achieved a substantial enrichment of various palladium isotopes: ^{102}Pd – up to 18 % (the natural content being 1 %), ^{104}Pd – up to 70 % (11.4 %), and ^{105}Pd – up to 60 % (22.33 %).

Thus, the method of selective laser photoionisation is promising for the production of other rare isotopes for medicine.

References

1. Karlov N.V., Prokhorov A.M. *Usp. Fiz. Nauk*, **118**, 583 (1976).
2. Karlov N.V., Krynetskii B.B., Mishin V.A., Prokhorov A.M. *Usp. Fiz. Nauk*, **127**, 59383 (1979).
3. *Trudy FIAN*, **114** (Moscow: Nauka, 1979).
4. Krynetskii B.B., Mishin V.A., Prokhorov A.M. *Zh. Prikl. Spektr.*, **54**, 558 (1991); Preprint IOFAN, No. 70 (Moscow: 1990).
5. Letokhov V.S., Moore S.B. *Kvantovaya Elektron.*, **3**, 248 (1976) [*Sov. J. Quantum Electron.*, **6**, 129 (1976)].
6. Letokhov V.S., Mishin V.L., Puretzky A.A. *Progr. Quantum Electron.*, **5** (3), 139 (1977).
7. Ambartzumian R.V., Kalinin V.N., Letokhov V.S. *Pis'ma Zh. Eksp. Teor. Fiz.*, **13**, 305 (1971).
8. Yakovlenko S.I. *Kvantovaya Elektron.*, **25**, 971 (1998) [*Quantum Electron.*, **28**, 945 (1998)].
9. Yakovenko S.I. *Laser Part. Beams*, **16** (4), 541 (1998).
10. Yakovlenko S.I. *Adv. Laser Opt. Res.*, **1**, 53 (2002).
11. Letokhov V.S. *USSR Inventor's Certificate No. 784679; Byull. Izobret.*, (8), 308 (1982).
12. Mishin V.I., Fedoseyev V.N., Kluge H.J., Letokhov V.S., et al. *Nucl. Instrum. Meth., B*, **73** (4), 550 (1993).
13. Derzhiev V.I., Mushta V.M., Yakovlenko S.I. Method for Separating Ytterbium Isotopes, Russian Federation Patent RU 21198116C1; Russian Federation Inventor's Certificate No. 96111686/25; *Izobret.*, (28), 10 (1998).
14. Derzhiev V.I., Kuznetsov V.A., Mikhal'tsov V.A., Mushta V.M., Sapozhkov A.Yu., Tkachev A.N., Chaushanskii S.A., Yakovlenko S.I. *Kvantovaya Elektron.*, **23**, 771 (1996) [*Quantum Electron.*, **26**, 751 (1996)].
15. Derzhiev V.I., Kuznetsov V.A., Mikhal'tsov L.A., Mushta V.M., Sapozhkov A.Yu., Tkachev A.N., Chaushanskii S.A., Yakovlenko S.I. *Proc. Int. Conf. Lasers'96* (McLean, VA: STS Press, 1997) pp 441–448.
16. Derzhiev V.I., Egorov A.G., Il'in A.A., Kostritsa S.A., Kuznetsov V.A., Mikhal'tsov V.A., Mushta V.M., Polovtsev A.A., Sapozhkov A.Yu., Tkachev A.N., Chaushanskii S.A., Yakovlenko S.I. *Proc. II All-Russian Conf. on Physicochemical Processes in Selection of Atoms and Molecules* (Moscow: Atominform Central Research Institute, 1997) pp 57–61.
17. Derzhiev V.I., Kostritsa S.A., Kuznetsov V.A., Mikhal'tsov V.A., Mushta V.M., Sapozhkov A.Yu., Tkachev A.N., Chaushanskii S.A., Yakovlenko S.I. *Proc. II All-Russian Conf. on Physicochemical Processes in Selection of Atoms and Molecules* (Moscow: Atominform Central Research Institute, 1997) pp 83–85.
18. Derzhiev V.I., Kostritsa S.A., Kuznetsov V.A., Mikhal'tsov V.A., Mushta V.M., A.A., Sapozhkov A.Yu., Tkachev A.N., Chaushanskii S.A., Yakovlenko S.I. *Kvantovaya Elektron.*, **25**, 287 (1998) [*Quantum Electron.*, **28**, 278 (1998)].
19. Derzhiev V.I., Kuznetsov V.A., Mikhal'tsov L.A., Mushta V.M., Sapozhkov A.Yu., Tkachev A.N., Chaushanskii S.A. *Proc. SPIE Int. Soc. Opt. Eng.*, **3403**, 242 (1998).
20. Tkachev A.N., Yakovlenko S.I. *Kvantovaya Elektron.*, **23**, 860 (1996) [*Quantum Electron.*, **26**, 839 (1996)].
21. Tkachev A.N., Yakovlenko S.I. *Kvantovaya Elektron.*, **24**, 759 (1997). [*Quantum Electron.*, **27**, 740 (1997)].
22. Golyatina R.I., Tkachev A.N., Yakovlenko S.I. *Kvantovaya Elektron.*, **25**, 764 (1998) [*Quantum Electron.*, **28**, 744 (1998)].
23. Prokhorov A.M., Tkachev A.N., Yakovlenko S.I. *Dokl. Ross. Akad. Nauk*, **329**, 729 (1993).
24. Maiorov S.A., Tkachev A.N., Yakovlenko S.I. *Matem. Model.*, **6**, 13 (1994).
25. Mayorov S.A., Tkachev A.N., Yakovlenko S.I. *Laser Phys.*, **4** (3), 624 (1994).
26. Golyatina R.I., Tkachev A.N., Yakovlenko S.I. *Laser Phys.*, **7** (2), 449 (1997).
27. Golyatina R.I., Tkachev A.N., Yakovlenko S.I. *Kratk. Soobshch. Fiz. FIAN*, (1–2), 92 (1997).
28. Golyatina R.I., Tkachev A.N., Yakovlenko S.I. *Zh. Tekh. Fiz.*, **68**, 771 (1999).
29. Golyatina R.I., Tkachev A.N., Yakovlenko S.I. *Laser Phys.*, **8** (5), 1095 (1998).
30. Tkachev A.N., Yakovlenko S.I. *Kvantovaya Elektron.*, **20**, 1117 (1993) [*Quantum Electron.*, **23**, 972 (1993)].
31. Savel'ev V.V., Yakovlenko S.I. *Kvantovaya Elektron.*, **23**, 1020 (1996) [*Quantum Electron.*, **26**, 994 (1996)].
32. Savel'ev V.V., Yakovlenko S.I. *Kratk. Soobshch. Fiz. FIAN*, (11–12), 57 (1996).
33. Savel'ev V.V., Yakovlenko S.I. *Laser Phys.*, **7** (2), 437 (1997).
34. Savel'ev V.V., Yakovlenko S.I. *Kvantovaya Elektron.*, **24**, 939 (1997) [*Quantum Electron.*, **27**, 913 (1997)].
35. Golyatina R.I., Syts'ko Yu.I., Yakovlenko S.I. *Laser Phys.*, **8** (4), 860 (1998).
36. Yamaguchi H., Sasao N. *Proc. Intern. Symp. Adv. Nuclear Energy Res.* (Oarai, Japan, 1989) (Tokyo: JAERI, 1990) p. 129.
37. Sasao N., Yamaguchi H. US Patent US005110562A, filed Feb. 28, 1990. Date of Patent May 5, 1992.
38. Tkachev A.N., Yakovlenko S.I. *Kvantovaya Elektron.*, **32**, 164 (2002) [*Quantum Electron.*, **32**, 164 (2002)].
39. Derzhiev V.I., Dyakin V.M., Il'kaev R.I., Mikhal'tsov V.A., Selemir V.D., Sidorov I.I., Tkachev A.N., Chaushanskii S.A., Yakovlenko S.I. *Kvantovaya Elektron.*, **32**, 619 (2002) [*Quantum Electron.*, **32**, 619 (2002)].
40. Derzhiev V.I., Dyakin V.M., Il'kaev R.I., Mikhal'tsov V.A., Sapozhkov A.Yu., Selemir V.D., Sidorov I.I., Tkachev A.N., Chaushanskii S.A., Yakovlenko S.I. *Kvantovaya Elektron.*, **33**, 553 (2003) [*Quantum Electron.*, **33**, 553 (2003)].
41. Yakovlenko S.I. *Producing of ^{168}Yb of weighable amounts by AVLIS method and selective photo-ionization of palladium. Proc. SPIE Int. Soc. Opt. Eng, in press.*
42. Van Duijn E.J., Witte S., Zinkstok R., Hogervorst W. *Eur. Phys. J. D*, **19**, 25 (2002).
43. Parr A.C., Elder F.A. *J. Chem. Phys.*, **49** (6), 2665 (1968).
44. Kozlov M.G., Kotochigova S.A., Nikolaev V.N. *Opt. Spektrosk.*, **41**, 10 (1976).
45. Yi J., Lee J., Kong H.J. *Phys. Rev. A.*, **51** (4), 3053 (1995).

46. Lyabin N.A., Churkin A.D., Ugol'nikov S.A., Koroleva M.E., Kazaryan M.A. *Kvantovaya Elektron.*, **31**, 191 (2001) [*Quantum Electron.*, **31**, 191 (2001)].
47. Zherikhin A.N., Letokhov V.S., Mishin V.I., Belyaev V.P., Evtyunin A.N., Lesnoi M.A. *Kvantovaya Elektron.*, **8**, 1340 (1981) [*Sov. J. Quantum Electron.*, **11**, 806 (1981)].
48. Dorofeev S.N., Zhil'tsov V.I., Klimashina A.T., Mnuskin V.E., Mishin V.I., Nikiforov V.G., Trinchuk B.O., Tokareva A.N., Fedorov V.A. *Zh. Prikl. Spektrosk.*, **41**, 514 (1984).

Discussion of results with N.G. Basov (1964).